Biosensors and Bioelectronics 74 (2015) 939–946

Contents lists available at ScienceDirect

Biosensors and Bioelectronics

journal homepage: www.elsevier.com/locate/bios

Electrochemical DNA sensor for anthrax toxin activator gene *atxA*-detection of PCR amplicons

Ritu Das, Ajay K. Goel**, Mukesh K. Sharma, Sanjay Upadhyay*

Defence Research and Development Establishment, Jhansi Road, Gwalior 474002, India

ARTICLE INFO

Article history:
Received 12 May 2015
Received in revised form
15 July 2015
Accepted 28 July 2015
Available online 29 July 2015

Keywords:
Biosensor
Differential pulse voltammetry
DNA
Hybridization
Mercaptopropyl trimethoxy silane
PCR amplicons

ABSTRACT

We report the DNA probe functionalized electrochemical genosensor for the detection of *Bacillus anthracis*, specific towards the regulatory gene *atxA*. The DNA sensor is fabricated on electrochemically deposited gold nanoparticle on self assembled layer of (3-Mercaptopropyl) trimethoxysilane (MPTS) on GC electrode. DNA hybridization is monitored by differential pulse voltammogram (DPV). The modified GC electrode is characterized by atomic force microscopy (AFM), cyclic voltammetry (CV), and electrochemical impedance spectroscopy (EIS) method. We also quantified the DNA probe density on electrode surface by the chronocoulometric method. The detection is specific and selective for *atxA* gene by DNA probe on the electrode surface. No report is available for the detection of *B. anthracis* by using *atxA* an anthrax toxin activator gene. In the light of real and complex sample, we have studied the PCR amplicons of 303, 361 and 568 base pairs by using symmetric and asymmetric PCR approaches. The DNA probe of *atxA* gene efficiently hybridizes with different base pairs of PCR amplicons. The detection limit is found to be 1.0 pM (S/N ratio = 3). The results indicate that the DNA sensor is able to detect synthetic target as well as PCR amplicons of different base pairs.

1. Introduction

Bacillus anthracis, a Gram-positive, sporulating, rod-shaped aerobic bacterium is the causative agent of anthrax. It is found in the environment in spore form and is considered as a potential tool in biological warfare. Humans get environmental exposure through soil or contaminated products from infected animals, such as hides, hairs, wool and excreta. Most forms of the disease are lethal, and it affects both humans and other animals. Anthrax can enter the human body through the intestines (ingestion), lungs (inhalation), or skin (cutaneous) and causes distinct clinical symptoms based on its site of entry (Centers for disease control and prevention (CDC), 2001; Logan et al., 2011). The anthrax proteins and the capsule are considered primary virulence factors of bacterium. The toxin genes *pagA*, *cya*, and *lef* encoding the toxin component protective antigen (PA), edema factor (EF) and lethal factor (LF), respectively are located on plasmid pXO1 and the capsule gene *capB*, *capC*, *capA*, and *capD* are located on pXO2 plasmids (Mock and Fouet, 2001; Pilo and Frey, 2011; Young and Collier, 2007). In *B. anthracis*, the virulence gene regulator *atxA* (anthrax toxin activator), located on plasmid pXO1 controls expression of the anthrax toxin of pXO1 plasmid and poly-γ-D-glutamic acid capsule located on pXO2 (Bourgogne et al., 2003; Hoffmaster and Koehler, 1997; Hadjifrangiskou and Koehler, 2008; Fouet, 2010). AtxA is a capsule operon transcriptional activator, it controls the regulation of genes harbored by both virulence plasmids, in addition *atxA* controls the expression of chromosomal surface-layer genes, found between peptidoglycan and the capsule that completely covers the surface, and there is plasmid-plasmid and plasmid-chromosome cross talk (Drysdale et al., 2005; Fouet, 2010; Uchida et al., 1997). Thus *atxA* gene is considered as a global gene regulator, but not much research has been focused on the diagnosis of anthrax using *atxA* at gene level.

B. anthracis is detected by diverse methods including bacteriology, serology-immunoassays, PCR techniques involving amplification and sequencing of characteristic nucleic acids (Logan et al., 2011; Levine et al., 2002). In these methodologies the different analytical approaches have been studied for detection of anthrax. Dipicolinic acid, a main constituent of *B. anthracis* spore has been detected fluorescently and electrochemically (Tan et al., 2014; Farrow et al., 2013). Immunoassay detection of PA and LF toxins are reported using different analytical techniques such as electrochemical, optical, surface enhanced Raman scattering (Tang et al., 2009; Quinn et al., 2002; Boyer et al., 2007, Oh et al., 2011; Park et al., 2009; Stoddard et al., 2014). The PA selective peptide sequences have also been used for detection of anthrax (Huan et al., 2011). Specific *pag-gene* (PA) based detection of *B. anthracis*

* Corresponding author. Fax: +91 751 2341148.
** Corresponding author.
E-mail addresses: akgoel73@yahoo.co.uk (A.K. Goel), sanjayupad@rediffmail.com (S. Upadhyay).

http://dx.doi.org/10.1016/j.bios.2015.07.066
0956-5663/

using the capture probe (oligonucleotide) by differential pulse voltammetry (DPV), electrochemical impedance spectroscopy (EIS), and quartz crystal microbalance (QCM) (Hao et al., 2011; Kara et al., 2008; Pal and Alocilja, 2010) has been reported by using various nanostructure/nanoparticles. Nanopore sensing method has been utilized for label-free real time detection of anthrax lethal factor (Wang et al., 2014). Lanthanide based fluorescent sensors for anthrax has also been reported (Lee et al., 2013).

Molecular–based (DNA) diagnostics has been widely used in clinical, forensic and pathogen detection due to numerous advantages such as specificity, sensitivity and easy miniaturization (Drummond et al., 2003; Ferapontova, 2011; Goral et al., 2006; Lai et al., 2006; Pedrero et al., 2011, Das et al., 2014; Kowalczyk et al., 2015). The use of electrochemical DNA biosensor is a practical approach at gene level detection of anthrax. The utilization of various biomarker gene for diagnosis of *B. anthracis* has been reported (Hao et al., 2011; Kara et al., 2008; Pal and Alocilja, 2010). Different studies have been carried on *atxA* gene of *B. anthracis,* its use as a biomarker has wide applicability in the diagnosis of *B. anthracis*. It controls the expression of toxin genes by positive regulation of capsule gene and structural gene transcription of *B. anthracis.* Till date no reports are available for the detection of B. *anthracis* by using *atxA* gene.

Electrochemical genosensor is based on DNA hybridization principle for sequence specific detection (Idili et al., 2014; Cui et al., 2014). The development of electrochemical genosensor holds great promise towards diagnosis of inherited and microbiological diseases in connection with clinical analysis (Xiao et al., 2007; Campuzano et al., 2011; Chen et al., 2012). Detection of electrochemical DNA sensors in untreated biological matrices or unpurified PCR amplicons is very limited. Various approaches have been optimized for the detection of PCR amplified DNA, such as use of asymmetric PCR it amplifies ss-DNA which can be directly used for hybridization eliminating the denaturation step of PCR amplicon (Lai et al., 2006; Mix et al., 2009; Pedrero et al., 2011). The electrochemical DNA sensor for the detection of unpurified double stranded and denatured PCR amplicons have also been studied (Hao et al., 2011; Patterson et al., 2010; Pedrero et al., 2011; Sun et al., 2010; Tosar et al., 2010). Label-free electrochemical DNA biosensor by identifying factors controlling the direct transduction efficiency to detect oligonucleotides in a complex real samples consisting of PCR amplicon has been reported (Zhang et al., 2012).

Here, we report the fabrication of DNA probe functionalized electrochemical genosensor for sequence specific gene level detection of *B. anthracis,* using regulatory gene *atxA*. The crucial aspect of developed genosensor is the construction of the DNA recognition interface that will ensure high hybridization efficiency and decrease non-specific adsorption of single-stranded DNA. Electrochemical deposition of gold nanoparticle was performed on self-assembled layer of MPTS modified GC electrode for immobilization of thiol modified DNA probe complementary to the target DNA, methylene blue used as a redox probe which intercalate within the DNA and amplify the detection signal. The detection strategy involves both Differential Pulse Voltammetry (DPV) and Electrochemical Impedance Spectroscopy (EIS) measurement of modified electrode signal. We have optimized DNA surface density using chronocoulometric method (Steel et al., 1998). We have also studied the electrochemical DNA hybridization assay in PCR-amplified samples without any purification or pre-treatment of the samples using both symmetric and asymmetric PCR product.

2. Materials and methods

2.1. Chemicals & reagents

(3-Mercaptopropyl) trimethoxysilane(MPTS), 6-Mercapto-1-hexanol, 97% (MCH) Methylene Blue, Gold (III) chloride trihydrate ($HAuCl_4 \cdot 3H_2O$), Potassium ferrocyanide ($K_4Fe(CN)_6 \cdot 3H_2O$), potassium ferricyanide $K_3Fe(CN)_6$ were obtained from Sigma-Aldrich, Milwaukee, USA, the primers, probes and short targets of probes for *atxA* gene were custom synthesized from Sigma Aldrich India Pvt Ltd., Bangalore (India), dATP, dCTP, dGTP and dTTP and Taq polymerase were obtained from Sigma Aldrich, USA. All other chemicals used in the present studies were of molecular biology grade and all the reagents were prepared in MilliQ water. The solutions and glasswares were autoclaved prior to being used.

2.2. Bacillus anthracis genomic DNA and PCR

Genomic DNA was isolated from *B. anthracis* Sterne strain as per the procedure described earlier (Jackson et al., 1997). The DNA probe and target sequence of *atxA* gene used for the detection *B. anthracis* are, Probe: HS-$(CH_2)_6$-5′-GCTTTAAGGAGGTAGAAC-3′, Target: 5′-CGAAATTCCTCCATCTTG-3′. The detailed list of DNA capture probe for *B. anthracis*, primers and mismatch target sequences used for detection gene *atxA* are given in Table S1. The primers, probes and short targets of probes for *atxA* gene were designed on the basis of *atxA* gene sequence of *B. anthracis* (Gen Bank accession number L13841.1), and were custom synthesized from Sigma Aldrich India Pvt Ltd, Bangalore (India). The primers Atx 840-F and Atx-R amplify a 568 bp fragment, whereas the primers Atx1047-F and Atx-R amplify a 361 bp fragment of *B. anthracis*. PCR amplification of the target DNA was carried out using 200 μL PCR tube with a reaction mixture of 25 μL. Each of the reaction mixtures contained 1 × reaction buffer, 200 μmol/L each of dATP, dCTP, dGTP, dTTP and 1.5 mmol/L $MgCl_2$, 1 U of Taq polymerase, 10 × reaction buffer, 10 pmol of each primer for symmetric PCR and 10 pmol of forward and 1 pmol of reverse primer for asymmetric PCR, 100 ng DNA and milli-Q water up to 25 μL. The Cycling conditions for PCR (Biorad, USA) included an initial denaturation at 94 °C for 2 min, followed by 30 cycles of 1 min of denaturation at 94 °C, 1 min of primer annealing at 58 °C, 2 min of extension at 72 °C followed by final extension at 72 °C for 10 min. In control reaction, deionized water was added to reaction mixture instead of bacterial DNA. PCR products thus obtained were used in the study. To check the size of amplicons, PCR products were separated by electrophoresis on a 1.5% (*W/V*) agarose gel containing ethidium bromide (0.5 μg/mL). A 100 bp DNA ladder (Sigma) was loaded on gel as a molecular size standard.

PCR amplicons of *B.anthracis* (361 bp and 568 bp) were used to test the real applicability of DNA sensor by the DNA probe immobilized at electrode surface. We used both symmetric and asymmetric PCR amplicons. To generate an excess amount of single-stranded DNA targets, asymmetric PCR technique was employed by using the different ratio of forward and reverse primers.

2.3. Apparatus

The electrochemical measurements were carried out on a PGSTAT 302 from Autolab with GPES software (EcoChemie, The Netherlands). A conventional three-electrode system comprising glassy carbon (GC) electrode ($\Phi = 3$ mm) as working electrode after modification with MPTS and AuNP denoted as MPTS/Au NP/DNA, platinum wire as auxiliary electrode and Ag/AgCl electrode as a reference electrode are used for electrochemical measurements. Electrochemical impedance spectroscopy (EIS), Differential pulse voltammetry (DPV) and cyclic voltammetry (CV) were

performed in 10 mM phosphate buffer (pH 7.4). AFM images were obtained using NT-MDT NTEGRA platform.

2.4. Electrodeposition of AuNP on GC electrode

The GC electrode was polished to a mirror-like surface with 0.3 and 0.05 μm alumina slurry on microcloth pads and sonicated in ethanol and water. The cleaned GC electrode again cycled in 0.1 M H_2SO_4 (four times from 0 to 2.0 V) for activation of the electrode (Cesarino and Cavalheiro, 2008; Won et al., 2005). MPTS modified electrode was achieved by immersing in MPTS sol–gel solution for a certain time (2 h) to form a self-assembled sol–gel film. The sol solution was formed by previously reported method (Das et al., 2014) with slight modification. In brief, 6 μL of MPTS sol has been mixed with 4 mL distilled water and 600 μL 0.1 M HCl to achieve ~65.0 mM concentration of MPTS. The modified electrode was kept for drying for 2–4 h. On the modified GC electrode, electrochemical deposition of AuNPs was carried out in 1 mM $HAuCl_4$ containing 0.5 M H_2SO_4 with potentiostatic method at −0.2 V for 120 s. After electrodeposition of AuNPs on the MPTS modified GC electrode, it was gently washed with distilled water and dried at room temperature.

2.5. Immobilization of DNA probe

Briefly, 4 μL of 10 μM thiolated ss-DNA probe against *atxA* gene in 10 mM phosphate buffer (pH 7.4) was dropped on AuNPs modified GC electrode and incubated for 1 h at 37 °C in humid environment. The ss-DNA probe modified GC electrode was rinsed with 10 mM phosphate buffer thoroughly, the electrode was then covered by 1 μL of 1.0 mM MCH solution for 30 min to obtain a well aligned ss-DNA/MCH modified electrode for its good recognition ability, followed by rinsing with water to remove unspecific adsorbed DNA probe and drying at room temperature (Scheme 1).

2.6. DNA hybridization assay and detection

The assay procedure was initiated by incubating the target DNA sequence with the ss-DNA probe modified GC electrode with different concentrations at 40 °C for 40 min to form ds-DNA. Further these ds-DNA modified electrodes were washed with distilled water and dried. Same procedure is followed with mismatch sequences, non specific sequences and PCR products. To study the hybridization reaction by differential pulse voltammogram (DPV) methylene blue (MB) was used as an electrochemical indicator (Kang et al., 2009). For the electrochemical measurements, the ss-DNA probe modified and ds-DNA (hybridized) GC electrode was immersed in 20 μM methylene blue (MB) for 5 min separately and is characterized by DPV in 10 mM phosphate buffer (pH 7.4).In both cases after accumulation of MB, the electrode was washed with 10 mM phosphate buffer thoroughly before recording the DPV in 10 mM phosphate buffer (pH 7.4).

In order to test the applicability with large base pairs, we challenged it with unpurified PCR amplicons of asymmetric and symmetric PCR product. The symmetric PCR products was thermally denatured before hybridization assay for the availability of ss DNA, by heating at 95 °C for 5 min. the amplicon strands reannealing was then retarded by cooling in ice bath for 5 min and subjected to electrochemical detection following the same procedure used of synthetic oligonucleotides.

3. Results and discussions

3.1. Electrochemical characterization of AuNPs modified GC electrode

A schematic representation of fabrication procedure of developed DNA sensor is illustrated in Scheme 1. A self assembled monolayer of MPTS sol–gel was formed on the glassy carbon electrode by dipping bare GC electrode in ~65 mM MPTS sol solution. Followed by drying it for 2 h, a controlled electrochemical deposition of AuNPs was carried out which was used for immobilization of thiol-modified DNA probe and hybridization on the GC electrode surface, increasing the sensitivity and loading capability of the sensor. The modified GC electrode was characterized by cyclic voltammogram (CV). The CVs of bare GC, MPTS modified GC and AuNPs/MPTS modified electrodes were recorded in 5 mM $[Fe(CN)_6^{3-/4-}]$ in phosphate buffer (Fig. 1). A pair a well defined redox peaks was observed on the bare GC electrode (Fig. 1 curve a). After the modification with MPTS on GC electrode no peak was observed suggesting that it hinders the electron transfer on the GC electrode for diffusion of ferricyanide toward the electrode surface (Fig. 1 curve b). After the electrodeposition of AuNPs, the peak current of $[Fe(CN)_6^{3-/4-}]$ increased and the peak to peak potential separation (ΔEp) decreased slightly, indicating a better redox behaviors of $[Fe(CN)_6^{3-/4-}]$ on the AuNPs modified electrode (Fig. 1 curve c). The average value of the electroactive surface area of the unmodified and Au NPs modified electrodes were calculated according to the Randles–Sevick equation (Bard and Faulkner, 2000):

$$I_p = 2.69 \times 10^5 A D^{1/2} n^{3/2} \gamma^{1/2} C$$

where n is the number of electrons participating in the redox reaction, A is the area of the electrode (cm^2), D is the diffusion coefficient of the molecule in solution ($cm^2\ s^{-1}$), C is the concentration of the probe molecule in the bulk solution ($mol\ cm^{-3}$), and γ is the scan rate ($V\ s^{-1}$). The electroactive surface area for

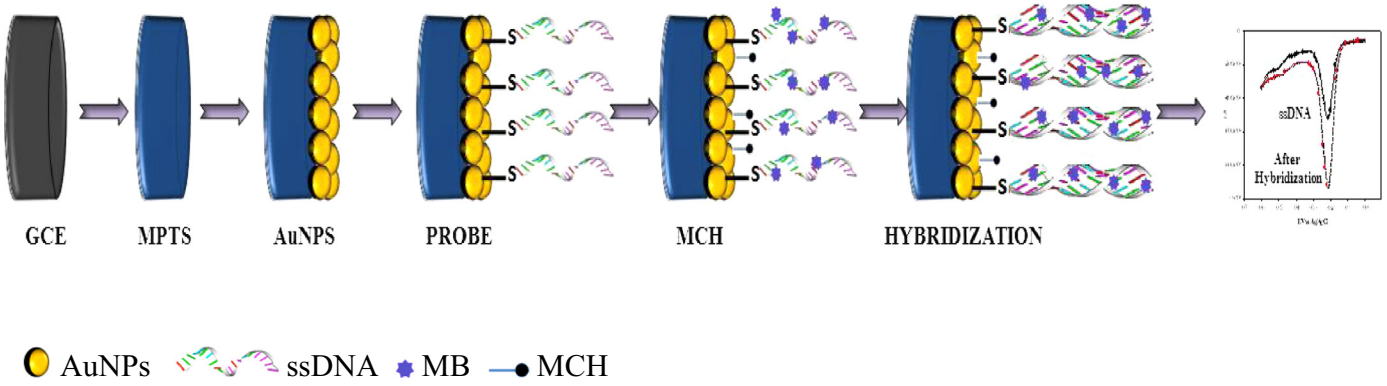

Scheme 1. The schematic representation of the MPTS-AuNPs modified GC platform for the electrochemical DNA sensor for *B. anthracis* detection.

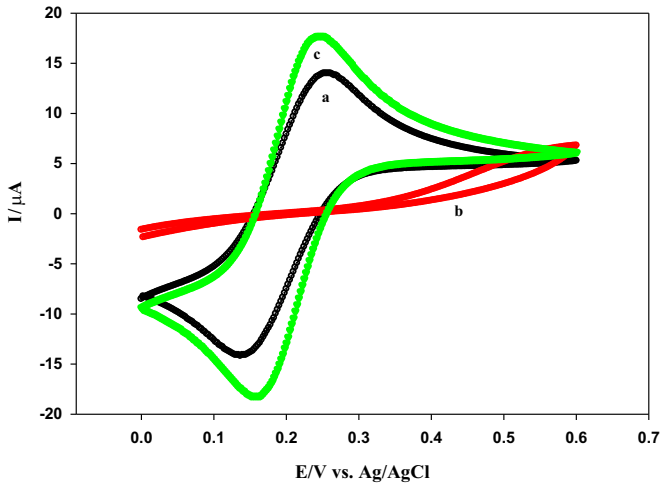

Fig. 1. Cyclic voltammograms in 5 mM $Fe(CN)_6^{3-/4-}$ containing 0.1 M KCl at 10 mV/s of different modified GC electrode (scan range 0.0–0.6 V vs Ag/AgCl): (a) Bare GC electrode (b) MPTS modified GC electrode, and (c) AuNPs-MPTS/GC electrode.

unmodified GC and Au NPs modified GC electrodes were $(1.20 \pm 0.3) \times 10^{-5}$ cm^2, and $(1.6 \pm 0.2) \times 10^{-5}$ cm^2 ($n=3$) respectively. The Au NPs modified electrode exhibit the high electroactive surface area and it provides an electron conducting pathways to the MPTS modified electrode surface. We have also characterized it by electrochemical impedance spectroscopy (EIS) data were given in Fig. S1 (supplementary data).

3.2. SEM and AFM characterization of modified electrode

The surface morphologies of blank GC (inset of Fig. S2) and AuNPs modified GC can be seen in Fig. S2 which clearly illustrates the uniform deposition of AuNPs on the electrode surface. This could significantly increase the electrode surface area improving the electron transfer ability, and also enhance the probe loading capacity. Fig. 2 shows AFM images obtained upon MPTS, AuNPs electrodeposition and ss-DNA probe immobilization. Fig. 2 (a) shows MPTS sol–gel formed on the GC electrode and it covers the whole surface area of the electrode. In Fig. 2b the topography of the image clearly shows the presence of AuNPs on GC electrode after electrodeposition and it also covers the whole surface of the electrode and their z-scale height is ~20 nm. The electrodeposition of AuNPs indicates the interaction between thiol groups of MPTS on GC electrode and morphology changed on the surface. After the immobilization of ss-DNA probe on the AuNPs modified GC electrode change in morphology of the electrode is observed and its Z-scale height is increased to ~50 nm (Fig. 2c). It confirms the proper ss-DNA immobilization on the electrode surface and is observed in Z-scale height change.

3.3. DNA surface density on modified electrode

The quantification of DNA coverage density on electrode surface was calculated from the electrostatic interaction of cationic redox molecule hexaammineruthenium(III) chloride $[Ru(NH_3)_6]^{3+}$ with the anionic DNA backbone by CV or chronocoulometry (CC) response (Lao et al., 2005; Steel et al., 1998). The charge Q, as a function of time t in coulometry is given by the integrated Cottrell equation:

$$Q = 2nFAD_0^{1/2}C_0t^{1/2}/\pi^{1/2} + Q_{dl} + nFA\Gamma_0$$

Where n is the number of electrons per molecule for reduction ($n=1$), F is the Faraday constant ($F=$ 96485 C/eq), A is the electrode area ($A=$ 0.07 cm^2), D_0 is the diffusion coefficient (6.3×10^{-6} cm^2/s), C_0 is the bulk concentration (0.1 milimolar/cm^2), Q_{dl} is the capacitive charge (1.2 μC), and $nFA\Gamma_0$ is the charge from the reduction of adsorbed redox marker [Γ_0 (mol/cm^2)]. The Γ_0 is the surface excess and represents the amount of redox marker $[Ru(NH_3)_6]^{3+}$ confined near the electrode surface. The intercept at $t=0$ is the sum of the double layer charging and the surface excess terms (Fig S3). Assuming that the redox molecule provide saturated condition it means complete charge compensation of DNA by $[Ru(NH_3)_6]^{3+}$. The double layer capacitance

$$\text{Surface concentration of} \left[Ru(NH_3)_6\right]^{3+} \text{is, } \Gamma_{Ru} = Q/nFA$$

The DNA surface density is determined from the saturated surface excess from $[Ru(NH_3)_6]^{3+}$ as

$\Gamma_{DNA} = \Gamma_{Ru}(z/m)(N_A)$ where Γ_{DNA} is the DNA probe surface density (mol/cm^2), m is the number of bases in DNA probe ($m=18$ base pair), z is the charge on redox marker, and N_A is Avogadro's number. The surface densities obtained is $(1-10) \times 10^{12}$ molecules/cm^2. If DNA probe surface densities are more, it may cause steric limitations on the surface for complete hybridization.

3.4. Electrochemical performance of DNA sensor with synthetic DNA target

The electrochemical performance of the DNA sensor was monitored by hybridization of ss-DNA probe against *atxA* gene with different concentration of synthetic target of ss-DNA sequence. The optimal hybridization time and temperature for DNA hybridization was 40 min at 40 °C (detailed data presented in the supplemental information Figs. S4 and S5). Fig. 3a shows the differential pulse voltammogram (DPV) of reductive signals obtained due to intercalation of MB with the ss-DNA/AuNPs/MPTS/GC (*atxA* gene probe modified electrode) and after hybridization with different concentrations of synthetic target ss-DNA sequence. The reductive signal of MB increased gradually with increase in concentration of target concentration. MB intercalate with the ss-DNA and ds-DNA in a different ways between the base pairs, insertion into the minor and major groove (Das et al., 2014; Henry et al., 2010; Kang et al., 2009). The adsorption of MB on to the electrode surface is very less due to the presence of ss-DNA immobilized in the electrode surface, MB can interact with ss-DNA by electrostatic binding between cationic MB and anionic DNA and due to the prolonged time immobilization of ss-DNA, the MB-DNA intercalation is more prominent then surface adsorption so the current monitored in the reduction signal can be considered due to MB-DNA intercalation. (Li et al., 2011; Tichoniuk et al., 2008; Xu et al., 2011; Zhu et al., 2008). The reductive signals obtained from MB carries electron transport from ds-DNA to electrode surface. It reveals the hybridization of target DNA with the immobilized probe, more ds-DNA adsorbed on the electrode surface more will be the accumulation of MB on the DNA and increase in reduction peak current is observed. The difference of peak current before and after hybridization was plotted with the logarithmic value of target sequence concentrations (Fig. 3b). A proportional relationship was observed between logarithmic of target concentration and the difference in DPV peak currents in a linear range from 1×10^{-11} to 1.0×10^{-9} M ($n=3$) and a linear regression equation was calculated as

$$I = 0.180log[DNA] + 0.923$$

Where log [DNA] is the target sequence concentration. The detection limit was 1.0 pM (S/N ratio=3, 3σ method where σ is standard deviation of the blank current, $n=3$). It demonstrates a feasible molecular detection of *B. anthracis* by using *atxA* gene DNA probe and is further used for the study with PCR amplicon.

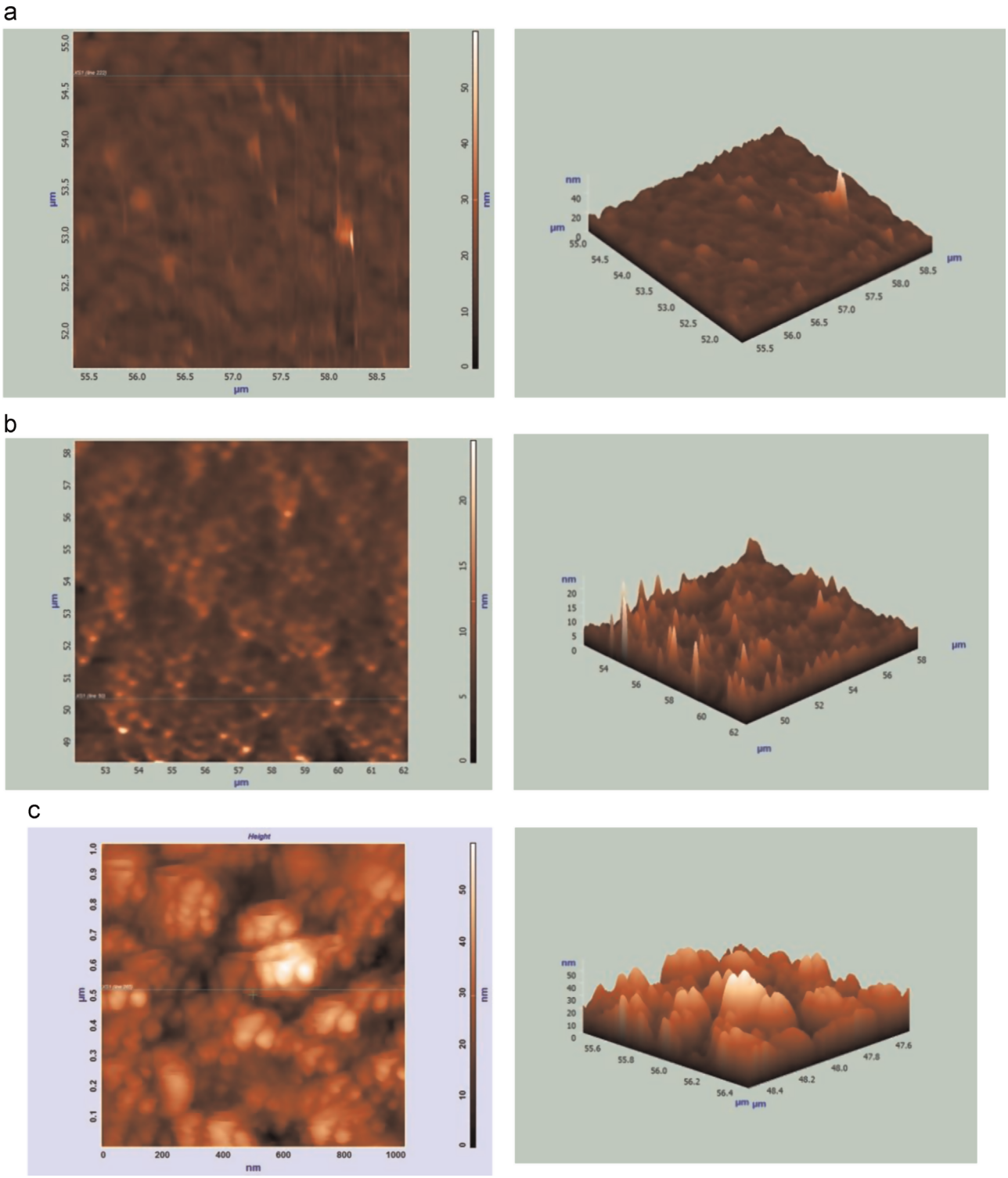

Fig. 2. Topography AFM images of MPTS modified GC electrode (image a), Au NPs-MPTS/GC electrode (image b), ss-DNA/Au NPs/MPTS/GC electrode (image c), and their respective 3D image with scale height.

3.5. Selectivity and reproducibility of the DNA biosensor

The selectivity and specificity is a crucial factor in DNA biosensor. We evaluated these factors by complementary synthetic target sequence (18 base pairs 100% of *atxA* complementary gene target), three base mismatch (80% of *atxA* complementary gene target) and nine base mismatch (50% of *atxA* complementary gene target) under the same optimized hybridization condition and other electrochemical parameters. Fig. 4a represents the bar graph between difference in current and percentages of mismatch target sequences. The current difference for 80% and 50% mismatch sequences is significantly low as compared to 100% complementary target sequence. The relative standard deviation (R.S.D.) obtained was 0.2% ($n=3$). These results demonstrate that the hybridization is not achieved with mismatch sequences and is highly specific for complementary sequences. To test the selectivity of the *atxA* gene probe, biosensor was studied with different genes of *B. anthracis* species protective antigen (PA), edema factor (EF) and lethal factor

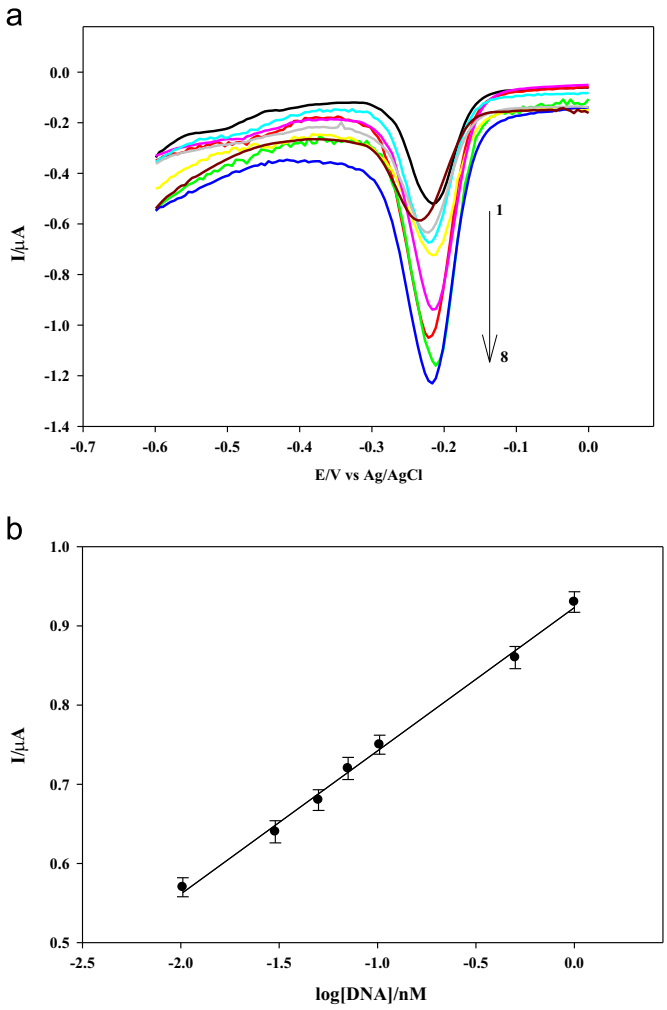

Fig. 3. (a) Differential pulse voltammograms (DPV) of methylene blue on ss-DNA probe-modified GC electrode and after hybridization with different concentrations of target sequences. Concentrations of target sequences from 1 to 8 are in increasing order 0.01, 0.03, 0.05, 0.07, 0.1, 0.5, 1.0, and 2.0 nM. (b) Calibration curve of the sensor response to target sequence, plot of difference of peak current from DPV before and after hybridization versus logarithm of target sequence concentration.

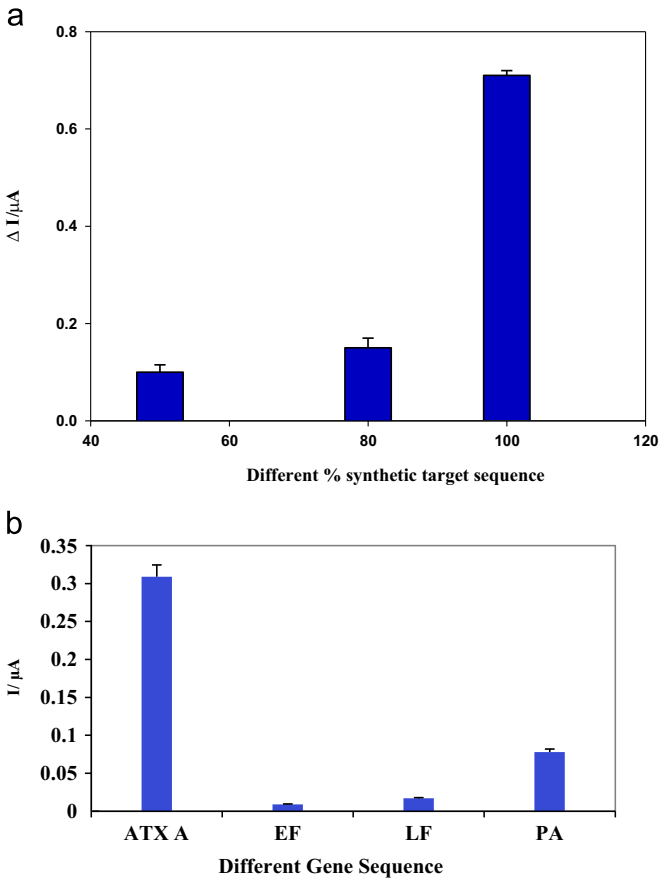

Fig. 4. (a) Bar graph represents the difference in DPV current with different percentage mismatch synthetic target sequences with concentration of 1.0 nM ($n=3$, R.S.D.$=0.2\%$). (b) Bar graph represents the difference in DPV current with different gene sequences *atxA* (anthrax toxin activator gene), EF (edema factor gene), LF (lethal factor gene) and PA (protective antigen), each having concentration of 1.0 nM ($n=3$, R.S.D.$=0.25\%$).

(LF). As shown in Fig. 4b, no significant difference in current is observed for PA, EF and LF genes, it showed that *atxA* DNA probe is highly selective for its complementary target. The relative standard deviation (R.S.D.) obtained was 0.25% ($n=3$). Overall, these results shows that the present DNA probe is highly specific and selective towards complementary target sequence only.

Reproducibility is an important factor for the performance of biosensor, it was investigated using three different electrodes fabricated independently under the same conditions to detect 1.0×10^{-9} M target DNA. The relative standard deviation (R.S.D.) obtained was 1.2%, reveals the acceptable reproducibility of the biosensor.

3.6. Detection of PCR amplicons

In order to detect the complex sample we selected the PCR amplicons of 303 bp, 361 bp and 568 bp that could be sensed by immobilized DNA probe. In all the PCR amplicons *atxA* gene sequence resides between them. We obtained symmetric and asymmetric PCR amplicons for hybridization with probe. In asymmetric PCR, both forward and reverse primers are in different concentrations which generate ss-DNA targets, helping in eliminating the denaturation step (Hao et al., 2011; Mix et al., 2009; Pedrero et al., 2011). The symmetric PCR amplicons (303 bp) fragments are procured containing specific region of probe. It was denatured by heating it in boiling water bath for 5 min, and immediate cooling in ice bath for 5 min. The ss-DNA target sequence is obtained and is hybridized under the optimized condition with DNA probe on the electrode surface. We have also used purified and unpurified PCR amplicons of 303 bp. The developed sensor performed well despite the fact that amplicons is much larger than the synthetic target. The curve I represents the probe and curve II & III represents unpurified and purified amplicons after hybridization Fig. 5a (303 bp). Reductive current of MB is less in unpurified state when compared with purified, it may be due to the presence of some interfering species. Further, we have used the asymmetric PCR amplicons to avoid the denaturation process of larger base pairs (361 bp & 568 bp). By this protocol obtained PCR amplicons are ss-DNA. These PCR amplicons of 361 bp and 568 bp hybridizes under the optimized condition with DNA probe on the electrode surface. Fig. 5b and c represents the DPV of 361 & 568 base pairs respectively after hybridization with DNA probe. We found that, hybridization with asymmetric PCR amplicons could also selectively identify the *B. anthracis atxA* gene in larger base pairs. We have demonstrated the selective identification of PCR amplicons (symmetric and asymmetric PCR amplicons) in larger base pairs with present DNA sensor.

3.7. Response in serum samples

We conducted DNA hybridization experiments with serum

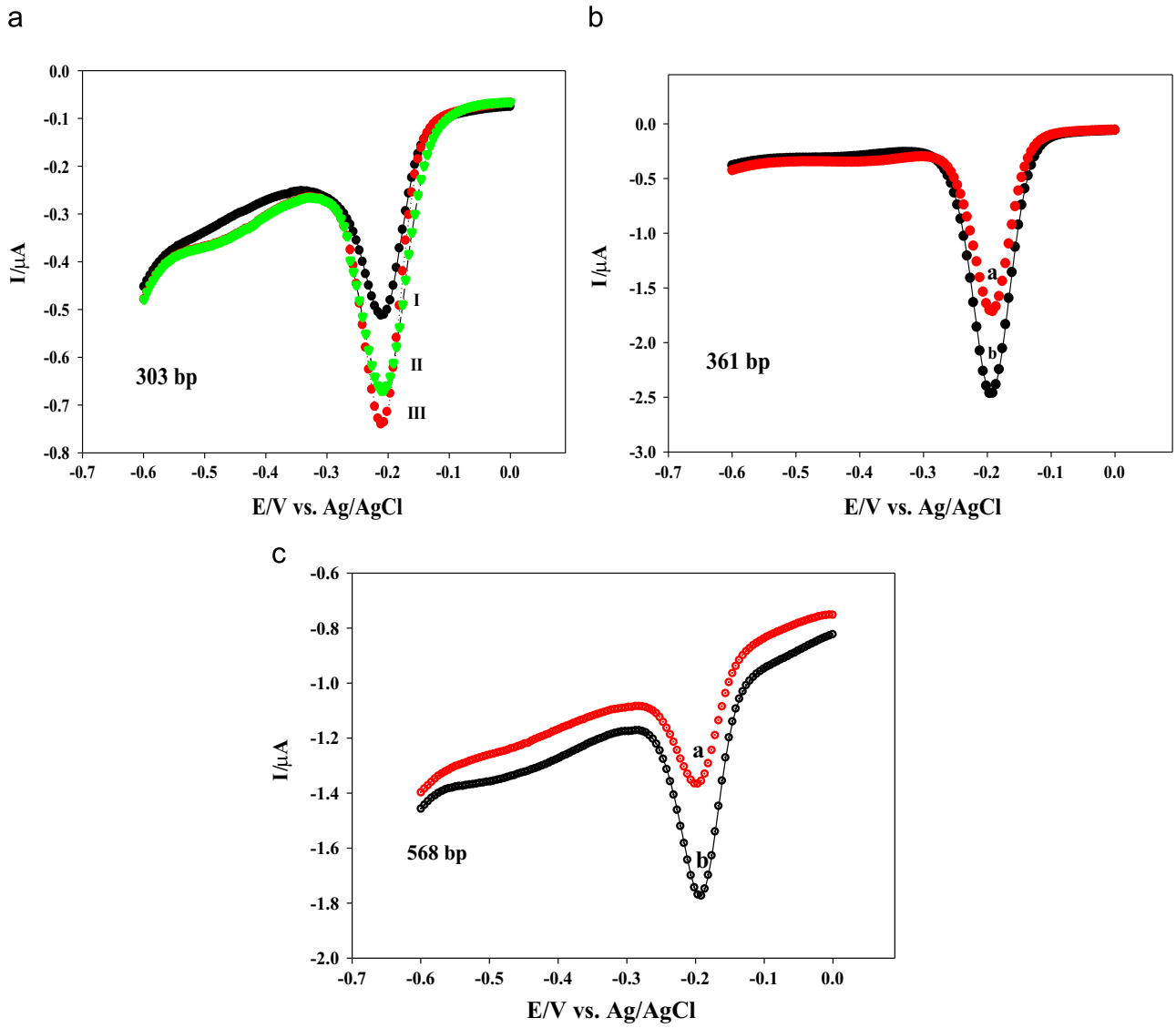

Fig. 5. DPV response of symmetric and asymmetric PCR amplicons of different base pairs. (a) DPV response of symmetric PCR amplicons (303 bp), curve I is ss-DNA probe, curve II is DNA hybridization with unpurified PCR amplicons (303 bp) and curve III is DNA hybridization with purified PCR amplicons (303 bp). (b) DPV response of asymmetric PCR amplicons (361 bp) ratio of forward and reverse primers is 10:1, curve a is ss-DNA probe, and curve b is DNA hybridization with PCR amplicons (361 bp) (c) DPV response of asymmetric PCR amplicons (568 bp) ratio of forward and reverse primers is 10:1, curve a is ss-DNA probe, and curve b is DNA hybridization with PCR amplicons (568 bp).

samples to see the matrix effect on response (Cash et al., 2009). The measurements were studied with synthetic complementary target spiked in diluted 1:10 serum with phosphate buffer (10 mM, pH 7.4). The synthetic complementary target (0.05 nM) spiked serum sample hybridized under optimized condition and found that small difference in peak current is obtained it may be due to the matrix effect (Fig. S6). This study indicates the feasibility of DNA biosensor in complex matrix. The DPV response is monitored in phosphate buffer solution and then diluted serum sample. We observed the slight variation in DPV peak potential it may be due to the matrix effect.

4. Conclusion

We have explored the regulatory gene *atxA* as a DNA probe in electrochemical DNA sensor for the detection of *B. anthracis*. The *atxA* gene as DNA probes (thiolated probe) immobilized on gold nanoparticle deposited MPTS modified GC electrode. The surface of the modified electrode is characterized by AFM, CV, and EIS. The DNA hybridization is monitored by differential DPV. The linear range was found from 1×10^{-11} to 1.0×10^{-9} M ($n=3$) and the detection limit was 1.0 pM (S/N ratio = 3). We have quantified ss-DNA probe surface densities on the electrode surface and it was found $(1-10)\times10^{12}$ molecules/cm^2. Furthermore, the specificity and selectivity of the DNA sensor was also studied and it demonstrates good specificity and selectivity with different gene sequences. The DNA electrochemical sensor was applied for the detection of PCR amplicons of different base pairs of *B.anthracis*. The results indicated that the DNA sensor could easily hybridized with different base pairs of PCR amplicons. It is a new approach for the detection of *B. anthracis* by using *atxA* gene as DNA probes. It can be seen that the present study offers good results concerning the detection of PCR amplicons of large base pairs. This approach can be further utilized for direct genomic DNA detection.

Acknowledgments

We are grateful to Director, DRDE Dr. Lokendra Singh and Head,

Biosensor Development Division, Dr. V.K.Rao for providing necessary facilities to carry out research work.

Appendix A. Supplementary material

Supplementary data associated with this article can be found in the online version at http://dx.doi.org/10.1016/j.bios.2015.07.066.

References

Bard, A.J., Faulkner, L.R., 2000. Electrochemical Methods: Fundamentals and Applications. John Wiley, New York.

Bourgogne, A., Drysdale, M., Hilsenbeck, S.G., Peterson, S.N., Koehler, T.M., 2003. Infect. Immun. 71, 2736–2743.

Boyer, A.E., Quinn, C.P., Woolfitt, A.R., Pirkle, J.L., Mcwilliams, L.G., Stamey, K.L., Bagarozzi, D.A., Hart Jr., J.C., Barr, J.R., 2007. Anal. Chem. 79, 8463–8470.

Campuzano, S., Kuralay, F., Lobo-Castanon, M.J., Bartosik, M., Vyavahare, K., Palecek, E., Haake, D.A., Wang, J., 2011. Biosens. Bioelectron. 26, 3577–3583.

Cash, K.J., Heeger, A.J., Plaxco, K.W., Xiao, Y., 2009. Anal. Chem. 81, 656–661.

Centers for disease control and prevention (CDC), 2001. Human anthrax associated with an epizootic among livestock-North Dakota, 2000. MMWR Morb.Mortal Wkly Rep. 50, 677.

Cesarino, I., Cavalheiro, E.T.G., 2008. Mater. Res. 11, 465–469.

Chen, X., Hong, C.Y., Lin, Y.H., Chen, J.H., Chen, G.N., Yang, H.H., 2012. Anal. Chem. 84, 8277–8283.

Cui, H.F., Cheng, L., Zhang, J., Liu, R., Zhang, C., Fan, H., 2014. Biosens. Bioelectron. 56, 124–128.

Das, R., Sharma, M.K., Rao, V.K., Bhattacharya, B.K., Garg, I., Venkatesh, V., Upadhyay, S., 2014. J. Biotechnol. 188, 9–16.

Drummond, T.G., Hill, M.G., Barton, J.K., 2003. Nat. Biotechnol. 21, 1192–1199.

Drysdale, M., Bourgogne, A., Koehler, T.M., 2005. J. Bacteriol., 5108–5114.

Farrow, B., Hong, S.A., Romero, E.C., Lai, B., Coppock, M.B., Deyle, K.M., Finch, A.S., Stratis-Cullum, D.N., Agnew, H.D., Yang, S., Heath, J.R., 2013. ACS Nano 7, 9452–9460.

Ferapontova, E.E., 2011. Curr. Anal. Chem. 7, 51–62.

Fouet, A., 2010. Res. Microbiol. 161, 735–742.

Goral, V.N., Zaytseva, N.V., Baeumner, A.J., 2006. Lab Chip 6, 414–421.

Hadjifrangiskou, M., Koehler, T.M., 2008. Microbiology 154, 2501–2512.

Hao, R.Z., Song, H.B., Zuo, G.M., Yang, R.F., Wei, H.P., Wang, D.B., Cui, Z.Q., Zhang, Z., Cheng, Z.X., Zhang, X.E., 2011. Biosens. Bioelectron. 26, 3398–3404.

Henry, O.Y.F., Perez, J.G., Sanchez, J.L.A., O'Sullivan, C.K., 2010. Biosens. Bioelectron. 25, 978–983.

Hoffmaster, A.R., Koehler, T.M., 1997. Infect. Immun. 65, 3091–3099.

Huan, T.N., Ganesh, T., Han, S.H., Yoon., M.Y., Chung, H., 2011. Biosens. Bioelectron. 26, 4227–4230.

Idili, A., Amodio, A., Vidonis, M., Feinberg-Somerson, J., Castronovo, M., Ricci, F., 2014. Anal. Chem. 86, 9013–9019.

Jackson, P.J., Walthers, E.A., Kalif, A.S., Richmond, K.L., Adair, D.M., Hill, K.K., Kuske, C.R., Andersen, G.L., Wilson, K.H., Hugh-Jones, M., Keim, P., 1997. Appl. Environ. Microbiol. 63, 1400–1405.

Kang, D., Zuo, X., Yang, R., Xia, F., Plaxco, K.W., White, R.J., 2009. Anal.Chem. 81, 9109–9113.

Kara, P., Meric, B., Ozsoz, M., 2008. Electroanalysis 20, 2629–2634.

Kowalczyk., A., Wagner, B., Karbarz, M., Nowicka, A.M., 2015. Sens. Actuators B: Chem. 208, 220–227.

Lai, R.Y., Lagally, E.T., Lee, S.H., Soh, H.T., Plaxo, K.W., Heeger, A.J., 2006. Proc. Natl. Acad. Sci. 103, 4017–4021.

Lao, R.J., Song, S.P., Wu, H.P., Wang, L.H., Zhang, Z.Z., He, L., Fan, C.H., 2005. Anal. Chem. 77, 6475–6480.

Li, F., Han, X., Shufeng, 2011. Biosens. Bioelectron. 26, 2619–2625.

Lee, I., Oh, W.K., Jang, J., 2013. J. Hazard. Mater. 252–253, 186–191.

Levine, S.M., Perez-Perez, G., Olivares, A., Yee, H., Hanna, B.A., Blaser, M.J., 2002. J. Clin. Vaccine Immunol. 40, 4360–4362.

Logan, N.A., Hoffmaster, A.R., Shadomy, S.V., Stauffer, K.E., 2011. In: Versalvoic, J., Carroll, K.C., Funke, G., Jogensen, J.H., Landry, M.L., Warnock, D.W. (Eds.), Manual of Clinical Microbiology Vol. 1. ASM Press, Washington, D.C.

Mix, M., Reske, T., Duwensee, H., Flechsig, G.U., 2009. Electroanalysis 21, 826–830.

Mock, M., Fouet, A., 2001. Annu. Rev. Microbiol. 55, 647–671.

Oh, B.N., Lee, S., park, H.Y., Baeg, J.O., Yoon, M.Y., Kim, J., 2011. Analyst 136, 3384.

Pal, S., Alocilja, E.C., 2010. Biosens. Bioelectron. 26, 1624–1630.

Patterson, A., Caprio, F., Vallée-Bélisle, A., Moscone, D., Plaxco, K.W., Palleschi, G., Ricci, F., 2010. Anal. Chem. 82, 9109–9115.

Park, H.R., Go, H., Kalme, S., Mane, R., Han, S., Yoon, M., 2009. Anal. Chem. 81, 4280–4284.

Pedrero, M., Campuzano, S., Pingarron, J.M., 2011. Anal. Methods 3, 780–789.

Pilo, P., Frey, J., 2011. Infect.Gene. Evolut. 11, 1218–1224.

Quinn, C.P., Semenova, V.A., Elie, C.M., Romero-Steiner, S., Greene, C., Li, H., Stamey, K., Steward-Clark, E., Schmidt, D.S., Mothershed, E., 2002. Emerg. Infect. Dis. 8, 1103–1110.

Steel, A.B., Herne, T.M., Tarlov, M.J., 1998. Anal.Chem. 70, 4670–4677.

Stoddard, R.A., Quinn, C.P., Schiffer, J.M., Boyer, A.E., Goldstein, J., Bagarozzi, D.A., Soroka, S.D., Dauphin, L.A., Hoffmaster, A.R., 2014. J. Immun. Methods 408, 78–88.

Sun, W., Qin, P., Gao, H., Li, G., Jiao, K., 2010. Biosens. Bioelectron. 25, 1264–1270.

Tan, H., Ma, C., Chen, L., Xu, F., Chen, S., Wang, L., 2014. Sens. Actuators B: Chem. 190, 621–626.

Tang, S.X., Moayeri, M., Chen, Z.C., Harma, H., Zhao, J.Q., Hu, H.J., Purcell, R.H., Leppla, S.H., Hewlett, I.K., 2009. Clin. Vaccine Immunol. 16, 408–413.

Tichoniuk, M., Ligaj, M., Filipiak, M., 2008. Sensors 8, 2118–2135.

Tosar, J.P., Branas, G., Laiz, J., 2010. Biosens. Bioelectron. 26, 1205–1217.

Uchida, I., Makino, S., Sekizaki, T., Terakado, N., 1997. Mol. Microbiol 23, 1229–1240.

Wang, L., Han, Y., Zhou, Wang, G., Guan, X., 2014. ACS Appl. Mater. Interfaces 6, 7334–7339.

Won, M.S., Rahman, M.A., Kwon, N.H., Shankaran, D.R., Shim, Y.B., 2005. Electroanalysis 24, 2231–2238.

Xiao, Y., Qu, X., Plaxco, K.W., Heeger, A.L., 2007. J. Am. Chem. Soc. 129, 11896–11897.

Xu, H., Gao, S., Hou, F., 2011. Curr. Phys. Chem. 1, 7–10.

Young, J.A., Collier, R.J., 2007. Annu. Rev. Biochem. 76, 243.

Zhang, Q.D., March, G., Noel, V., Piro, B., Reisberg, S., Tran, L.D., Hai, H.V., Abadia, E., Nielsen, P.E., Sola, C., Pham, M.C., 2012. Biosens. Bioelectron. 32, 163–168.

Zhu, L., Zhao, R., Wang, K., Xiang, H., Shang, Z., Sun, W., 2008. Sensors 8, 5649–5660.